Lattice Models and Puzzles for Dual Weak symmetric Grothendieck Polynomials

Elisabeth Bullock, Noah Caplinger, Ariana Chin, Nyah Davis, Gahl Shemy

August 6, 2021

Abstract

We construct a solvable lattice model for the dual weak symmetric Grothendieck polynomials given by Pylyavskyy and Lam in [6] in hopes of using such a model to prove related properties of these polynomials, including Cauchy identities and branching rules. We also consider a similar lattice model construction for the weak symmetric Grothendieck polynomials in hopes of proving a Cauchy identity given by Yeliussizov [12], concluding with a negative result. Moreover, we expand on the work done by Pylyavskyy and Yang in [10] and by Zinn-Justin in [13] by giving boundary conditions for a proposed lattice model for the Littlewood Richardson coefficients of the dual weak symmetric Grothendieck polynomials, via an MS puzzle construction.

Contents

1 Introduction

Arising from quantum field theory, lattice models are tools that found their original use in modeling particle interactions in thin sheets of matter. These models consist of a finite grid where each vertex is given an

orientation of arrows on its adjacent edges, meant to reflect chemical bonds between molecules. Beyond just their utility in theoretical physics, however, lattice models have proven to be powerful tools in mathematics due to their ability to represent important polynomial functions, their bijective correspondence with ubiquitous combinatorial objects, and their ability to provide straightforward proofs to known identities that have otherwise complicated constructions. See [2] for more details.

Given a lattice model, we can assign weight functions to our vertices, known as *Boltzmann weights*, such that the partition function of the lattice model is a polynomial. Interestingly, a class of symmetric polynomials known as Grothendieck polynomials, which were first introduced by Lascoux and Schützenberger in [7] as polynomial representatives for Schubert classes in K-theory, can also be represented by lattice models using a specific choice of Boltzmann weights. Much work has already been done on constructing lattice models for certain symmetric polynomials (for examples, see [1] for the Schur polynomial and [9] for the refined dual Grothendieck polynomial). This paper expands on this prior work by constructing a lattice model whose partition function evaluates to the dual weak symmetric Grothendieck polynomial introduced in [6].

Besides representing special symmetric polynomials, lattice models can also be used to prove important identities relating to these polynomials, including Cauchy identities and branching rules. In Section 4, we use our lattice model construction to prove a branching rule for the dual weak symmetric Grothendieck polynomials, adding to the branching formulas given in [12]. In Section 5, we discuss difficulties with constructing a lattice model proof for a Cauchy identity involving the weak symmetric Grothendieck polynomials. Although we conclude the Section with a negative result, we explore the possibility of relaxing some of the conditions considered to get the desired lattice model proof, taking inspiration from [3].

We conclude by once again considering the dual weak symmetric Grothendieck polynomials, this time through the lens of puzzles. Puzzles were originally introduced by Knutson, Tao, and Woodward in [5] as combinatorial objects which count Littlewood-Richardson coefficients. Section 6 is dedicated to exploring the puzzles and Littlewood-Richardson coefficients associated with our polynomials of study. Specifically, we explore a new hexagon tile introduced by Pylyavskyy and Yang in [10] used to count the Littlewood-Richardson coefficients for the dual weak symmetric Grothendieck polynomials. Finally, we describe a process of converting a tiled puzzle with hexagons into boundary conditions and vertices of a lattice model, with hopes that a choice of spectral parameters and Boltzmann weights will allows us to obtain the Littlewood-Richardson coefficient via this lattice model.

Acknowledgements

2 Preliminaries

Before proving the main result of our paper, we define some necessary terms and give descriptions of the most important polynomials in our study.

2.1 Young Tableaux

The symmetric polynomials we discuss in this paper are generated over specifications of Young tableaux, which we focus on in this subSection. Understanding Young tableaux requires us first to understand *partitions*.

Definition 2.1. *A **partition** λ is a string $(\lambda_1, \ldots, \lambda_m)$ of weakly decreasing nonnegative integers $\lambda_1 \geq \lambda_2 \geq \cdots \geq \lambda_m$. If λ has m entries in its string, we say that the **length** of λ is $len(\lambda) = m$, and we denote the **cardinality** of λ by $|\lambda| = \sum_{i=1}^{m} \lambda_i$.*

To each partition λ we associate a *Young tableau* of shape λ.

Definition 2.2. *A **Young diagram** of shape λ is a collection of boxes such that row i of the tableau contains λ_i boxes, and all rows are left-justified.*

If μ and λ are two partitions, we say that $\mu \subseteq \lambda$ if and only if for each i, $\mu_i \leq \lambda_i$. If the partitions are not of the same length, we pad out the partition of shorter length with entries of zero until the two partitions have the same length.

Given partitions μ and λ such that $\mu \subseteq \lambda$, we can now define *skew partitions* and *skew Young diagrams*.

Definition 2.3. *A **skew partition** λ/μ is a set of two partitions λ, μ such that $\forall i$, $\mu_i \leq \lambda_i$. A **skew Young diagram** of shape λ/μ is a Young diagram of shape λ with missing boxes corresponding to a Young diagram of shape μ. Often times we shade in the boxes corresponding to μ in the skew diagram λ/μ.*

Example. *If we let $\lambda = (4, 2)$ and $\mu = (1, 0)$, then the skew tableau of shape $(4, 2)/(1, 0)$ is given by*

with the dotted lines representing the Young tableau of the partition $(1, 0)$ taken out of the Young tableau of $(4, 2)$.

Since any Young diagram of shape λ can be viewed as a skew diagram of shape λ/μ with $\mu = \emptyset$, we hereafter will only consider skew diagrams.

Fix an n that is greater than or equal to the number of rows in the skew diagram for λ/ν.

Definition 2.4. *A **skew Young tableau** of shape λ/μ is a filling of the skew diagram of shape λ/μ with numbers in $[n]$.*

We are now equipped to define several variations of skew Young tableaux that will prove useful in our study of lattice models in Section 3 and in our study of puzzles in Section 6.

Definition 2.5. *A **semistandard Young tableau** of shape λ/μ is a Young tableau of shape λ/μ such that the rows have weakly increasing entries, and columns have strictly increasing entries.*

Example. *Let $\lambda = (4, 2)$ and $\mu = (1, 0)$. We fix $n = 3$. One possible semistandard Young tableau under these restrictions is given by*

Definition 2.6. *A **valued-set tableau** (VST) of shape λ/μ is a semistandard Young tableau of shape λ/μ with the additional possibility of removed edges between boxes that share the same entry in the same row. When an edge between boxes is removed, we only leave one entry in the enlarged box that remains.*

Example. *Continuing with the running example we have been using, let $\lambda = (4, 2)$, let $\mu = (1, 0)$, and fix $n = 3$. One possible valued-set tableau under these restrictions is given by*

Section 5 will require two more specifications of Young tableaux, so although they will not be immediately useful to us, we define them in this Section for completeness.

Again fix an n that is greater than or equal to the number of rows in the skew diagram for λ/μ.

Definition 2.7. *Let A, B be subsets of $[n]$. A **set-valued tableau** (SVT) of shape λ/μ is a Young tableau of shape λ/μ with entries given by subsets of $[n]$ such that rows are weakly increasing and columns are strictly increasing. This means that if A is in a box directly to the left of a box filled with B, then $\max(A) \leq \min(B)$, and if A is in a box directly above a box filled with B, then $\max(A) < \min(B)$.*

Example. *Let $\lambda = (4, 2)$, $\mu = (1, 0)$, and $n = 3$. One possible set-valued tableau under these restrictions is given by*

	12	2	23
23	3		

Definition 2.8. *Let A, B be subsets of $[n]$. A **multiset-valued tableau** (MSVT) of shape λ/μ is a Young tableau of shape λ/μ with entries given by multisubsets of $[n]$ such that rows are weakly increasing and columns are strictly increasing. This means that if A is in a box directly to the left of a box filled with B, then $\max(A) \leq \min(B)$, and if A is in a box directly above a box filled with B, then $\max(A) < \min(B)$.*

Example. *Let $\lambda = (4, 2)$, $\mu = (1, 0)$, and $n = 3$. One possible multiset-valued tableau under these restrictions is given by*

	1222	2	23
223	33		

2.2 Grothendieck Polynomials

Each polynomial to be discussed in this paper is generated over one of the specifications of a Young tableau defined above. We begin by defining the titular polynomial, the dual weak symmetric Grothendieck polynomial.

Definition 2.9. *Fix partitions $\mu \subseteq \lambda$ and an $n \in \mathbb{N}$ that is greater than or equal to the number of rows in the skew diagram of λ/μ. The **dual weak symmetric Grothendieck polynomial** [6] of shape λ/μ in n variables is a polynomial $j_{\lambda/\mu}(\underline{z}, \alpha)$ such that*

$$j_{\lambda/\mu}(\underline{z}, \alpha) = \sum_{T \in VST_{\lambda/\mu}} \alpha^{|\lambda/\mu| - |T|} \underline{z}^{wt(T)}$$

*where $VST_{\lambda/\mu}$ is the set of all valued set tableaux of shape λ/μ, and $\underline{z}$ is the vector $(z_1, \ldots, z_n)$. Each individual z_i is called a **spectral parameter**, and $\underline{z}$ is known as the **row spectral parameter**.*

Example. *Fix $\lambda = (3, 2)$, $\mu = (1, 0)$, and $n = 2$. We wish to compute $j_{\lambda/\mu}(z_1, z_2, \alpha)$.*

We first find all SSYT's of shape λ/μ with fillings in $[2]$ and get the following four possibilities:

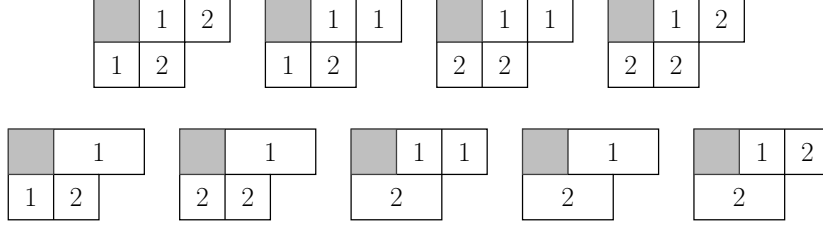|	1	2		1	1		1	1		1	2
1	2		1	2		2	2		2	2	

We now consider all of the possible VST's that result from our SSYT's. The possibilities are depicted below:

4

We therefore get that

$$j_{\lambda/\mu}(z_1, z_2, \alpha) = \sum_{T \in VST_{\lambda/\mu}} \alpha^{|\lambda/\mu|-|T|}(z_1, z_2)^{wt(T)}$$

$$= z_1^2 z_2^2 + z_1^3 z_2 + z_1^2 z_2^2 + z_1 z_2^3 + \alpha z_1^2 z_2 + \alpha z_1^2 z_2 + \alpha z_1 z_2^2 + \alpha^2 z_1 z_2 + \alpha z_1 z_2^2$$

$$= z_1^2 z_2^2 + (\alpha + z_1)z_1^2 z_2 + (\alpha + z_1)(\alpha + z_2)z_1 z_2 + (\alpha + z_2)z_1 z_2^2$$

From the dual weak symmetric Grothendieck polynomials we get another family of polynomials that are dual to our aforementioned family via the Hall inner product.

Definition 2.10. *Fix partitions $\mu \subseteq \lambda$ and an $n \in \mathbb{N}$ that is greater than or equal to the number of rows in the skew diagram of λ/μ. The **weak symmetric Grothendieck polynomial** of shape λ/μ in n variables is a polynomial $J_{\lambda/\mu}(\underline{z})$ such that*

$$J_{\lambda/\mu}(\underline{z}) = \sum_{T \in MSVT_{\lambda/\mu}} \underline{z}^{wt(T)}$$

where $MSVT_{\lambda/\mu}$ is the set of all multiset-valued tableaux of shape λ/μ, and $\underline{z}$ is the vector $(z_1, \ldots, z_n)$.

Definition 2.11. *Fix partitions $\mu \subseteq \lambda$ and an $n \in \mathbb{N}$ that is greater than or equal to the number of rows in the skew diagram of λ/μ. The **stable symmetric Grothendieck polynomial** of shape λ/μ in n variables is a polynomial $G_{\lambda/\mu}(\underline{z})$ such that*

$$G_{\lambda/\mu}(\underline{z}) = \sum_{T \in SVT_{\lambda/\mu}} \underline{z}^{wt(T)}$$

Given the symmetric polynomials defined in Definitions 2.9, 2.10, 2.11, a natural question introduced in Section 1 is whether there exist lattice models that represent these polynomials. We explore this question further in Section 3, after defining a lattice model and explaining how to construct one.

3   A Lattice Model for $j_{\lambda/\mu}$

In its most general form, a lattice model is a finite rectangular grid in which vertices on the intersections of the grid are assigned weights that depend on the vertex's adjacent edges. The ith row of the grid is indexed by a spectral parameter z_i, and the labels on the top and bottom rows of the model, as well as the first and last columns, are initially determined by a set of *boundary conditions*. Hereafter our edges will always be labeled with arrows, which can either point towards or away from a given adjacent vertex.

Additional rules may be imposed on the lattice, such as a condition called the *Ice Rule*, where the adjacent edges for a given vertex must obey the property that two of the edges are labeled with arrows pointing towards the vertex, and two are labeled with arrows pointing away from the vertex. The Ice Rule ensures some conservation of flow when the lattice model is used to model particles moving along the grid lines.

For the lattice models we discuss in this paper, the boundary conditions will always be determined by two partitions μ and λ such that $\mu \subseteq \lambda$. If $\mu = (\mu_1, \ldots, \mu_m)$ and $\lambda = (\lambda_1, \ldots, \lambda_m)$, we fix a partition $\rho = (m-1, \ldots, 1, 0)$ and consider the new partitions $\lambda + \rho$ and $\mu + \rho$. We then create binary strings of length $\lambda_1 + m$ for these new partitions by assigning a 1 to every (nonnegative) integer that appears in the updated
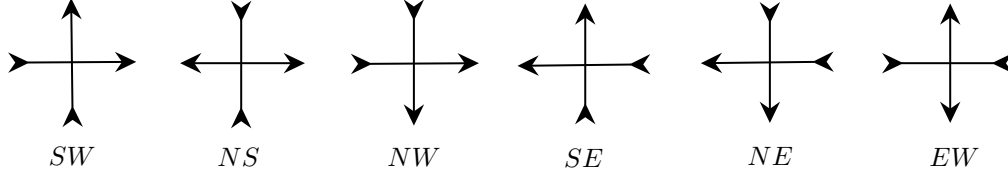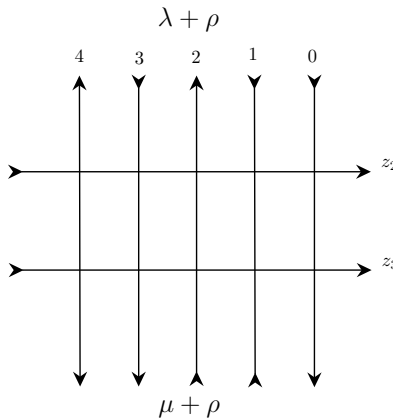
Figure 1: Admissible vertices in the Ice Model

partitions and a 0 to every integer that does not appear. Our lattice model is then forced to have $\lambda_1 + m$ columns, and if we fix an n that is greater than or equal to the number of rows in the skew diagram for λ/μ, we place n rows in our lattice model. We then define a *system* (a set of boundary arrows) as follows: for the vertices on the top (respectively, bottom) row, we put an outward facing (respectively, inward facing) arrow on the north (respectively, south) edge of the vertex wherever a 1 appears in the binary string, labeling our columns starting at 0 from the right. The arrows on both the left-most boundary and the right-most boundary point to the right, which translates to inward facing arrows on the left-most boundary and outward facing arrows on the right-most boundary.

Example. *Let $\lambda = (3,2)$, $\mu = (1,1)$, and let $n = 2$. Then $\lambda + \rho = (4,2)$ and $\mu + \rho = (2,1)$, so our lattice model will have outward facing arrows on columns 2 and 4 on the top row, and inward facing on columns 2 and 1 on the bottom row. The system is given by*

A *state* of the system is a filling of the lattice model fixed by a system with arrows on edges that do not belong to the boundary. We say that a state is *admissible* if each vertex is one of the six vertices depicted in Figure 1.

To each vertex as in Figure 1 in our lattice model we assign a weight function, called a *Boltzmann weight*, in terms of our spectral parameters. Given a filled in state S of the system , we say that the *weight of the state* is the product of all of the weights of the vertices of the state. Given a system $\mathfrak{S}$, we say that the *weight of the system* is the sum of all of the weights of the admissible states in the system.

Finally, we define the *partition function Z* of a lattice model to be the function that computes the weight of a system. Formally, if we are given partitions $\mu \subseteq \lambda$ and a fixed number of variables n, we get that

$$Z(\mathfrak{S}_{\lambda/\mu}(z_1, \ldots, z_n)) = \sum_{S \in \mathfrak{S}_{\lambda/\mu}} (z_1, \ldots, z_n)^{wt(S)}$$

Given these key definitions, we can now introduce the particular lattice model for our dual weak symmetric Grothendieck polynomials $j_{\lambda/\mu}(\underline{z})$. In [4], it is proved that there is a bijection between semistandard Young tableaux (SSYT) of shape λ/μ in n variables, and states in this lattice model. Although the lattice model is well-accepted, there is no written formal proof in the literature. Here, we state the full proof for the more generalized polynomials $j_{\lambda/\mu}(\mathbf{z}, \alpha)$, including the proof of the above bijection for completeness.

Theorem 3.1. *Given partitions* λ, μ,

$$j_{\lambda/\mu}(\underline{z}, \alpha) = Z\left(\mathfrak{S}_{\lambda/\mu}(\underline{z})\right),$$

where $\mathfrak{S}_{\lambda/\mu}$ is the system given by the weights in Figure 2 and boundary conditions listed immediately above these weights.

The proof of the lattice model for $j_{\lambda/\mu}(\mathbf{z}, \alpha)$ involves three steps. First, we will establish a bijection between SSYT and nonintersecting paths in the lattice model. Next, we will show the bijection between nonintersecting paths and states in the model. Together, these make up the proof of the aforementioned bijection. Lastly, we establish the actual equivalence of polynomials on either side of the bijection.

The lattice model for $j_{\lambda/\mu}(\mathbf{z}, \alpha)$ is constructed as follows. There are row spectral parameters z_i increasing from bottom to top. The columns are zero indexed from right to left. The model maintains the following boundary conditions.

Let m be the number of rows in λ and μ. We let the **rho shift** be $\rho = (m-1, ..., 1, 0)$.

- All arrows along the side boundaries face right (E).

- On the top boundary, $\lambda + \rho$ indicates the arrows facing up (N).

- On the bottom boundary, $\mu + \rho$ indicates the arrows facing up (N).

Finally, the model uses the following Boltzmann weights.

NW	NS	SW	NE	EW	SE
1	1	1	$\alpha + z_i$	z_i	0

Figure 2: The Boltzmann weights for L-vertices in row i in the $j_{\lambda/\mu}$ model.

Note that we may view this lattice model as a series of m paths whose endpoints are determined by $\mu + \rho$ and $\lambda + \rho$. Since the paths enter from the bottom and exit the top, we call this model a **top-bottom** lattice model. Additionally, we consider these m paths to be **left-up paths**, as they only flow left (W) and up(N) from start to end. See Figure 3 for an example of a valid lattice model state.

3.1 Bijection Between SSYT and Left-Up Paths

We construct a bijection between the semistandard Young tableaux of shape λ/μ with integers in $[n]$ and a choice of m nonintersecting left-up paths in the given lattice model. Define

$$\phi : \left\{ \begin{array}{l} \text{semistandard tableaux of form} \\ \lambda/\mu \text{ with integers in } [n] \end{array} \right\} \rightarrow \left\{ \begin{array}{l} \text{collections of } m \text{ nonintersecting} \\ \text{left-up paths in } \mathfrak{S}_{\lambda/\mu}(z_1, ..., z_n) \end{array} \right\}$$

as follows:

Given a semistandard tableau $\mathfrak{T}$ of form λ/μ with m rows (that is, λ is of length m), let $\mathfrak{T}_{(i,j)}$ be the value of the j-th block of row i of $\mathfrak{T}$. Additionally let ρ by the partition $\rho = (m-1, m-2, ..., 1, 0)$. Under ϕ, we construct the following paths:

- the path corresponding to the ith row starts at the bottom of column $\mu_i + \rho_i$ and ends at the top of column $\lambda_i + \rho_i$.

- from (vertical) lattice lines $(\mu_i + \rho_i) + (j - 1)$ to $(\mu_i + \rho_i) + j$, the path is going left on row spectral parameter $z_{\mathfrak{T}_{(i,j)}}$. After marking all such segments, the path can be uniquely completed using only vertical segments.

7

We may also define an inverse map ϕ^{-1}. Given a choice of m left-up non-intersecting paths from $\mathfrak{S}_{\lambda/\mu}$, the image under ϕ^{-1} gives:

- A semistandard Young tableau of shape λ/μ, such that:
  - the ith row of the tableau is determined by the path from $\mu_i+\rho_i$ to $\lambda_i+\rho_i$, according to the following rule: if the path goes left on (horizontal) line z_k from (vertical) lattice lines $(\mu_i + \rho_i) + (j-1)$ to $(\mu_i + \rho_i) + j$, then $\mathfrak{T}_{(i,j)} = k$

Example. *Let $\lambda = (3,2)$ and $\mu = (1,0)$. An example of a SSYT for λ/μ with values in $\{1,2\}$ is given on the left in Figure 3 with its corresponding lattice state on the right. Note that $\lambda + \rho = (4,2)$ and $\mu + \rho = (2,0)$.*
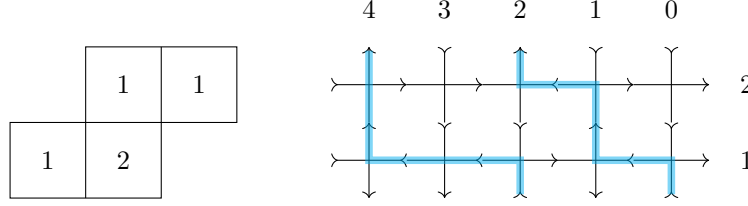

Figure 3: An SSYT of shape $(3,2)/(1,0)$ with labels in $\{1,2\}$ and its corresponding lattice state with paths indicated.

Lemma 3.1. ϕ *is well defined*

Proof. By construction, each of the m paths are completely determined by $\mathfrak{T}$. We need to show

1. Each path is going strictly up and left

2. There are no path intersections

(1) follows from the fact that each row in $\mathfrak{T}$ is weakly increasing, and that each horizontal path segment of unit length is uniquely determined by a single box in $\mathfrak{T}$.

(2) For the sake of contradiction, assume there is a path intersection between paths i and $i+1$. Let us observe the first (lowest) such intersection. Call the (vertical) lattice line at which the intersection takes place index $c = (\mu_i + \rho_i) + (a-1) = (\mu_{i+1} + \rho_{i+1}) + b$. Since these paths are intersecting, path i from lines c to $c+1$ must be at least as high as path $i+1$ from lines $c-1$ to c. Since $\rho_i = \rho_{i+1} + 1$, we have

$$(\mu_i + \rho_{i+1} + 1) + (a-1) = (\mu_{i+1} + \rho_{i+1}) + b$$

which implies that

$$\mu_i + a = \mu_{i+1} + b$$

Thus, the values of the paths at c correspond to the same column in $\mathfrak{T}$, and $\mathfrak{T}_{(i,\mu_i+a)} \geq \mathfrak{T}_{(i,\mu_{i+1}+b)}$, breaking the strictly increasing condition on columns of $\mathfrak{T}$. $\Rightarrow\Leftarrow$
Thus, no two adjacent paths can intersect and there are no path intersections. $\square$

Lemma 3.2. ϕ^{-1} *is well defined.*

Proof. By construction, each of the m rows are completely determined by the m paths in $\mathfrak{S}_{\lambda/\mu}$. We need to show

1. Each row is weakly increasing.

2. Each column is strictly increasing.

(1) follows from the fact that each path can only go up, and not down.
(2) For the sake of contradiction, assume that there is a column $c = \mu_i + a = \mu_{i+1} + b$ in $\mathfrak{T}$ not strictly

increasing. Then, there is some two adjacent rows i and $i+1$ such that the value of row i is $\geq$ the value of row $i+1$ on column c. Equivalently, $\mathfrak{T}_{(i,\mu_i+a)} \geq \mathfrak{T}_{(i+1,\mu_{i+1}+b)}$. Recall that $\rho_{i+1} = \rho_i - 1$. We have

$$\mu_i + a = \mu_{i+1} + b$$

which means that

$$(\mu_i + \rho_{i+1} + 1) + (a - 1) = (\mu_{i+1} + \rho_{i+1}) + b$$

So, the values in column c of $\mathfrak{T}$ exactly correspond to the row spectral parameters of the paths on column $(\mu_i + \rho_{i+1}) + b$ of the lattice model. Since $\mathfrak{T}_{(i,\mu_i+a)} \geq \mathfrak{T}_{(i+1,\mu_{i+1}+b)}$, path i is at least as high as path $i+1$ at this point. But, every point above path $i+1$ is within the region bounded by path $i+1$ on the left. Thus, path i has crossed path $i+1$, a contradiction. $\qquad\square$

Lemma 3.3. $\phi^{-1}\phi$ and $\phi\phi^{-1}$ is the identity.

Proof. All values $\mathfrak{T}_{(i,j)}$ and path height are conserved by construction. λ and μ are also conserved by adding and subtracting $\rho = (m-1, m-2, ..., 1, 0)$ when going to and from the lattice model, respectively. $\qquad\square$

3.2 Paths vs States

Our overarching proof strategy to show our lattice model describes $j_{\lambda/\mu}(z, \alpha)$ is as follows:

1. Establish a bijection between SSYT's and collections of non-intersecting paths in the model.

2. Show there is a bijection between collections of non-intersecting paths and non-zero states in the model (thereby giving a bijection between SSYT's and non-zero states)

3. Using the above bijection, show that

$$j_{\lambda/\mu}(\underline{z}, \alpha) = \sum_{T \in VST_{\lambda/\mu}} \alpha^{|\lambda/\mu|-|T|} \underline{z}^{wt(T)}$$

This Section is dedicated to step 2. We will do this in two parts: 1. show that every collection of non-intersecting paths completely determines a non-zero state (lemma 3.4) and 2. show that every non-zero state has a corresponding collection of non-intersecting paths (lemma 3.5)

Lemma 3.4. *The set of m non-intersecting paths completely determines a state of the lattice model $\mathfrak{S}_{\lambda/\mu}$. Moreover, every vertex not on a path is of the form EW, which has Boltzmann weight 1.*

Proof. The basic strategy of this proof is as follows: we scan the vertices in the first column, starting in the bottom left and moving upwards. In the process of the scan, we show that each vertex behaves nicely. Formally this is accomplished by ordering the vertices primarily by rightmost column, and secondarily by lowest row, and then inducting on the ordering. An example of this ordering on a 4×3 lattice is shown in Figure 4

We will prove the following statement by induction: for each vertex v, every non-path edge incident to v is either down or right.

If the first (ie left and bottom-most) vertex is on a path, The boundary conditions force S,E to be in and out respectively. The remaining path edge is out, so ICE forces the remaining non-path edge to be in (either down or right). Then the only non-path edges incident to the first vertex are either down or right, satisfying our claim.

If the first vertex is not on a path, then the boundary conditions specify E,S to be out arrows. ICE then forces N,W to be in arrows (See figure 5). Then every edge incident to v is either down or right. This constitutes the base case for our induction.
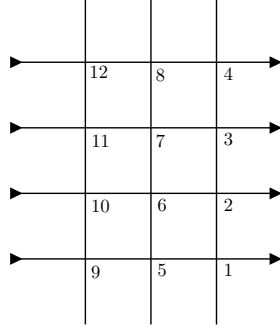
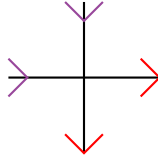Figure 4: The ordering of vertices given in the proof of lemma 3.4

Figure 5: Red indicates the boundary condition, purple are the deduced edges.

Let v denote some vertex and inductively assume that all vertices preceding v in the ordering satisfy our claim. That is, if w comes before v, then every non-path edge incident to w is either down or right. We will be referencing figure **??** frequently for casework. The blue arrows denote paths. It may be helpful to be looking at a copy of that as you read (I certainly am).

Case 1: A path goes through v. Then we are in cases β_4, β_1, β_3, or β_2 (See Figure 8).

β_4**:** The South edge of v is off-path, and is incident to the preceding vertex. Then the inductive hypothesis forces S to be outwards. Finally, S,W are out arrows, meaning ICE forces N,E to be in. Thus, all off-path edges incident to v are either down or right.

β_1**:** We know E is either a boundary edge (in which case it is right) or incident to a vertex preceding v in the ordering. Then we know E is right by induction, and because E,N are out arrows, ICE forces S,W to be in. Thus, all off-path edges incident to v are either down or right.

β_3**:** As before, we can conclude inductively that, S is down. Because S,N are out arrows, ICE forces E,W to be in.

β_2**:** Inductively we conclude, E is out. Because E,W are out arrows, ICE forces S,N to be in.

Case 2: v is not incident to a path. Then, by induction, S,E are both outwards facing, forcing N,W to be in arrows. Then all off-path edges incident to v are either down or right.

$\square$

We know from above that each (nonintersecting) path determines a (nonzero) state. So, the map

$$\psi : \{\text{non-intersecting paths}\} \rightarrow \{\text{nonzero states}\}$$

is well defined and clearly injective. We wish to show this is a bijection.

Lemma 3.5. *Every nonzero state has corresponding m non-intersecting paths.*

Proof. There are two things to prove.

1. Every up boundary edge on the bottom is connected to an up boundary edge on the top via a left-up path.

2. All such paths do not intersect

(1) For the sake of contradiction, suppose there is an up boundary edge on the bottom which is not connected to an up boundary edge on the top via a path. starting at this up boundary edge, we can follow edges up and left until the path stops.

Case 1: The path stops at a vertex that it has just hit from the south adjacent edge.
Because the path stops, both N and W must be inwards facing, but S is also inwards, which breaks ICE. This is a contradiction.
Case 2: The path stops at a vertex it has just hit from the east adjacent edge.
Again, because the path stops, both N and W are inward facing. But E is also inward facing breaking ICE. Again, this is a contradiction.

The proof is analogous for ends with broken paths, but with cases (N outwards) and (W outwards).

Assume for the sake of contradiction that two paths intersect. Because the paths move only up and left, we get SE which has weight 0, and our state has weight 0, a contradiction.

Then, we know that for each i, $\mu_i + \rho_i$ must connect to $\lambda_i + \rho_i$ (and vice versa) with exactly one path. So, we have m such non-intersecting paths. $\qquad\square$

3.3 Equivalence of Polynomials

Definition 3.1. *Given a semistandard tableau $\mathfrak{T}$, we let $VST(\mathfrak{T})$ be the set of valued-set-tableaux found by removing vertical lines from $\mathfrak{T}$ between boxes with the same entry*

Lemma 3.6. *Let $S \in \mathfrak{S}_{\lambda/\mu}$ be the state determined by a choice of m paths corresponding to semistandard tableau $\mathfrak{T}$ of type λ/μ. Then*

$$wt(S) = \sum_{T \in VST(\mathfrak{T})} \alpha^{|\lambda/\mu| - |T|} \underline{z}^{wt(T)}.$$

Where $wt(T)$ is a vector with i^{th} component the number of i's in T and $\underline{z}^{wt(\nu)} = \prod_{i=1}^{n} z_i^{wt(\nu)_i}$.

Proof. Note that for a given $T \in VST(\mathfrak{T})$, $|\lambda/\mu| - |T|$ is exactly the number of edges removed to get from $\mathfrak{T}$ to T (as each edge removed reduces the number of blocks by one). Thus, the degree of α for any particular valued-set-tableau ν is the number of edges omitted from the original young diagram of shape λ/μ.

Let $a_{r1}, a_{r2}, ..., a_{rn}$ denote the number of consecutive i-blocks on row r. Let T_i denote the ith row of T. Let

$$R_i = \sum_{L \in VST(T_i)} \underline{z}^{wt(L)}$$

be the summation over all VSTs for row i of T. Then,

$$T_r = \prod_{i=0, a_{ri} \neq 0}^{n} z_i(\alpha + z_i)^{a_{ri}-1}$$

since every nonzero block i must contribute at least one z_i, and every further adjacent i-block adds a factor of $(\alpha + z_i)$, the choice of omitting the edge (α) or including it (z_i). Thus,

$$\sum_{\nu \in VST(\mathfrak{T})} \alpha^{|\lambda/\mu| - |\nu|} \mathbf{z}^{wt(\nu)} = \prod_{r=1}^{m} T_r = \prod_{r=1}^{m} \prod_{i=0, a_{ri} \neq 0}^{n} z_i(\alpha + z_i)^{a_{ri}-1}$$

as each choice of edge inclusion is independent over rows.

Now, we check equivalence to the lattice model path corresponding to $\mathfrak{T}$. Indeed, we have only two nontrivial weights: z_i and $(\alpha+z_i)$, for NW and NS respectively. For the consecutive i-blocks of length a_{ri}, the path will hit NW once (when leaving z_i) and NS will be hit $a_i - 1$ times (path continues on z_i). So, this block contributes $z_i(\alpha + z_i)^{a_{ri}-1}$ to the product. So, for row r, our path will generate $\prod_{i=0,a_{ri}\neq0}^{n} z_i(\alpha + z_i)^{a_{ri}-1}$. Moreover, by Lemma 3.4, every vertex not on the path has weight 1. Thus, the lattice model is

$$wt(S) = \prod_{p=1}^{m} T_p = \prod_{p=1}^{m} \prod_{i=0,a_{pi}\neq0}^{n} z_i(\alpha + z_i)^{a_{pi}-1}$$

and we have

$$wt(S) = \sum_{T \in VST(\mathfrak{T})} \alpha^{|\lambda/\mu|-|T|} \underline{z}^{wt(T)}$$

$\square$

Theorem 3.2. *Given partitions λ, μ,*

$$j_{\lambda/\mu}(\underline{z}, \alpha) = \sum_{S \in \mathfrak{S}_{\lambda/\mu}} wt(S)$$

Proof. From the above lemma,

$$wt(S) = \sum_{T \in VST(\mathfrak{T})} \alpha^{|\lambda/\mu|-|T|} \underline{z}^{wt(T)}.$$

Since we know a bijection from nonzero states $S \in \mathfrak{S}_{\lambda/\mu}$ to non-intersecting paths (Section 3), and non-intersecting paths to semistandard tableaux (Section 2), we have the following:

$$\sum_{S \in \mathfrak{S}_{\lambda/\mu}} wt(S) = \sum_{\mathfrak{T} \in T} \sum_{v \in VST(\mathfrak{T}_{\lambda/\mu})} \alpha^{|\lambda/\mu|-|T|} \underline{z}^{wt(v)} = j_{\lambda/\mu}$$

where $T_{\lambda/\mu}$ is the set of all semistandard tableaux of form λ/μ. $\square$

4 Remarks on Our Lattice Model

Given our lattice construction from Section 3, we can now prove a number of interesting identities and facts about our model. We begin by proving that our model is *solvable*, a highly desirable property.

4.1 Solvability and the Yang-Baxter Equation

One of the powerful techniques of statistical mechanics is the Yang-Baxter equation, which allows us to extract functional equations satisfied by the partition function from geometric manipulations of the lattice. A lattice model satisfying a Yang-Baxter equation is called *solvable*. In this Section, we show that our j-model is solvable: in fact, it satisfies both row and column Yang-Baxter equations of RTT type. We can then use the row Yang-Baxter equation to give an easy proof of the symmetry of the j_λ polynomials, which was originally proven by [6] using commutation properties of operators. This symmetry is harder to see from the tableaux definition, but falls neatly out of the solvability of the j_λ model.

Consider an additional set of rotated, or diagonal, vertices that also follow the Ice rule. We call these R-vertices, in keeping with the literature. As with the vertices in Figure 2, we may assign Boltmann weights to these R-vertices, where now a vertex weight depends on the spectral parameters of the two rows it attaches to. In Figure 6, we give a set of such weights, viewing the i strand as the one travelling SW to NE and the j strand as that travelling NW to SE.

Proposition 4.1. *Together with the weights in Figure 2, the R-vertex weights in Figure 6 satisfy the following row Yang-Baxter equation: fixing boundary arrow conditions $\alpha, \beta, \gamma, \delta, \epsilon,$ and η, the partition functions of the*
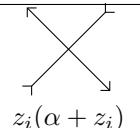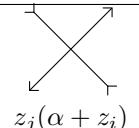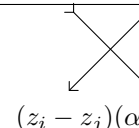
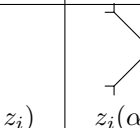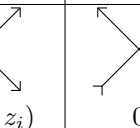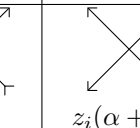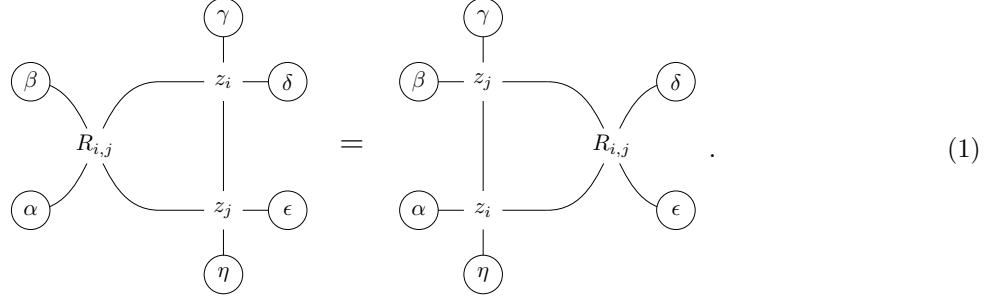| R_1	R_2	R_3	R_4	R_5	R_6
$z_i(\alpha + z_i)$	$z_j(\alpha + z_i)$	$(z_i - z_j)(\alpha + z_i)$	$z_i(\alpha + z_i)$	0	$z_i(\alpha + z_j)$

Figure 6: The row R-vertex weights for the j_λ model.

following two states are equal, where we have labelled the two j_λ model vertices with their spectral parameter.

$$\tag{1}$$

Proof. Since each vertex must conserve flow because of the Ice Rule, we must have the same number of in and out arrows on the boundary, that is, 3 of each. This reduces to $\binom{6}{3} = 20$ cases, which may be checked by hand. □

We may then use a *train argument* to reprove the symmetry of the $j_{\lambda/\mu}$ polynomials using the lattice model.

Proposition 4.2. *For all λ/μ, the polynomial $j_{\lambda/\mu}(z_1, ..., z_n; \alpha)$ is symmetric in the z_i.*

Proof. Since the symmetric group is generated by simple reflections, it suffices to show that the j polynomial is symmetric in z_i and z_{i+1}. Consider the lattice model with boundary conditions the same as $j_{\lambda/\mu}$, except with a single R vertex attached to rows i and $i+1$ on the right hand side, where condition that the side boundary arrows point right now appears on the outside of the R-vertex. Zooming in on rows i and $i+1$, this model looks like:
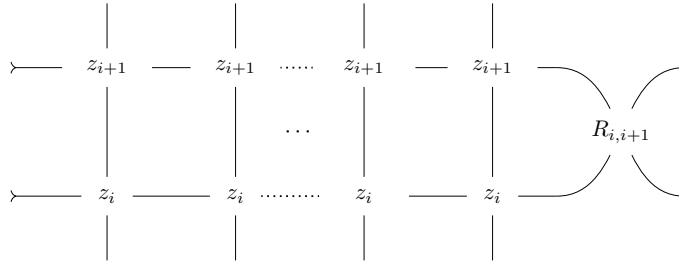
Since there is one option for the R-vertex (namely type R_4), the partition function of this system is $z_i(\alpha + z_i) \cdot j_{\lambda/\mu}(\boldsymbol{z})$. Using Proposition 4.1, we can push the R-vertex (like a train through a tunnel of columns) to the other side of the model, where it pops out on the left boundary, and the partition functions of these two systems (as well as any stop along the way) must be equal.

13
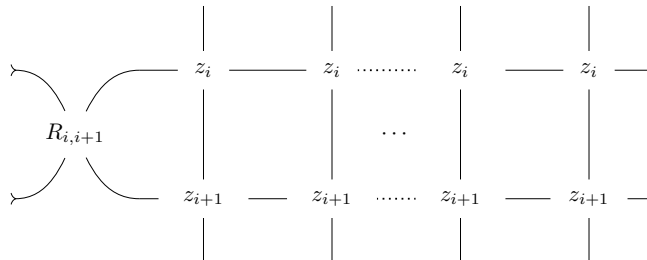
This process only affects rows i and $i+1$, which we see above. Considering the partition function, there is again only one option for the R-vertex, which must be an R_4. However, in this model, the parameters z_i and z_{i+1} have been switched on the remaining rectangle, so this partition function gives $z_i(\alpha + z_i) \cdot j_{\lambda/\mu}(z_1, ..., z_{i+1}, z_i, ..., z_n)$. Thus, since the R-vertex had the same weight on both sides, cancelling it off gives that $j_{\lambda/\mu}(\boldsymbol{z})$ is symmetric in z_i and z_{i+1}. $\square$

Even though our model does not have column parameters, we may still ask if there are analogous R-vertex weights for swapping columns. While the resulting weights we found are less interesting polynomials, we see that under the path interpretation, the non-zero vertices in Figure 7 are those that send paths straight up, preserving the boundary condition, rather than giving us relations between $j_{\lambda/\mu}$ polynomials for different skew shapes λ/μ.
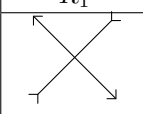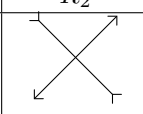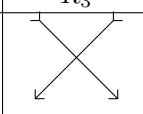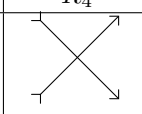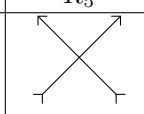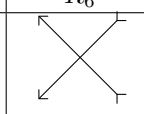
R_1	R_2	R_3	R_4	R_5	R_6
1	1	1	0	1	0

Figure 7: The column R-vertex weights for the j_λ model.

Proposition 4.3. *Together with the weights in Figure 2, the R-vertices in Figure 7 satisfy the following column Yang-Baxter equation: fixing boundary arrow conditions $\alpha, \beta, \gamma, \delta, \epsilon$, and η, the partition functions of the following two states are equal, where we have labelled the two j_λ model vertices with their spectral parameter.*
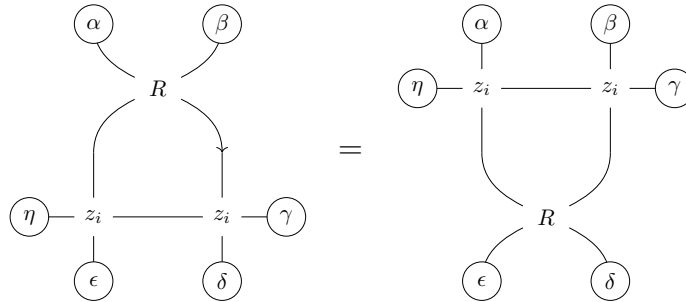
Proof. As for the row Yang-Baxter equation, there are only 20 cases of boundary arrows, which may be easily checked by hand. $\square$

4.2 Branching Rule

In this Section we give a recursive formula, or branching rule, for the dual weak symmetric Grothendieck polynomials. Motivated by the well-known branching rule for Schur polynomials given in [8], we show that we can express $j_{\lambda/\mu}$ as a sum over dual weak symmetric Grothendieck polynomials over certain partitions contained in λ/μ with entries in one less variable.

Fix λ and μ to be partitions as before with the property that $\mu \subseteq \lambda$, and consider a partition ν such that $\mu \subseteq \nu \subseteq \lambda$. In addition, fix a number of variables n such that $n \geq m$, where $m = len(\lambda)$. We say that $\mu \preceq \nu$ if the skew tableau for ν/μ is a *horizontal strip*, that is, if ν/μ has at most one box in each column of its skew tableau. This means that if we set $\nu = (\nu_1, \ldots, \nu_m)$ and $\mu = (\mu_1, \ldots, \mu_m)$, then $\mu \preceq \nu$ if and only if $\nu_{i+1} \leq \mu_i \leq \nu_i$ for each $1 \leq i \leq m-1$, and $\mu_m \leq \nu_m$.

Example. *Let $\nu = (3, 3, 1)$, and let $\mu = (2, 1, 0)$. Then $\mu \npreceq \nu$, since, for instance, $\nu_2 > \mu_1$. The Young tableau of shape ν/μ is*

We see that the resulting tableau is not a horizontal strip, as the third column contains two white boxes.

On the other hand, if we let $\nu = (3, 2, 1)$ and let $\mu = (2, 1, 0)$, then we do have that $\mu \preceq \nu$, and the Young tableau ν/μ is given by

which has only one white box in each column, as desired.

Similarly, we define $\preceq_{n-1}$ as follows: $\nu \preceq_{n-1} \lambda$ if and only if $\lambda_{i+n} \leq \nu_i \leq \lambda_i$ for $i \leq m - n - 1$, and $\nu_i \leq \lambda_i$ for $m - n \leq i \leq m$. Notice that by this definition, we have that $\nu \preceq_{n-1} \lambda$ if and only if the skew tableau for λ/ν has at most $n - 1$ boxes in a given column.

Proposition 4.4.

$$j_{\lambda/\mu}(z_1, \ldots, z_n) = \sum_{\mu \preceq \nu \preceq_{n-1} \lambda} j_{\lambda/\nu}(z_2, \ldots, z_n) z_1^{m-k} (1 + z_1)^{|\nu/\mu| - m + k}$$

where k gives the number of $i \in [m]$ such that $\nu_i = \mu_i$.

Proof. We decompose each VST of shape λ/μ filled with numbers $\{1, \ldots, n\}$ into two smaller VSTs, one of shape ν/μ filled with 1's and one of shape λ/ν filled with numbers $\{2, \ldots, n\}$. Since every value in the VST of ν/μ is a 1, in particular we know that every column of the VST of ν/μ has at most one box, such that $\mu \preceq \nu$. Similarly, since λ/ν is filled with $\{2, \ldots, n\}$, then each column of the VST of λ/ν must have at most $n - 1$ boxes, allowing us to conclude that $\nu \preceq_{n-1} \lambda$.

For each VST of shape λ/μ containing a ν/μ orientation of ones, we consider all possible VSTs that stem from that placement of ones. That is,

$$j_{\lambda/\mu}(z_1, \ldots, z_n) = \sum_{T \in \text{VST}(\lambda/\mu)} \underline{z}^{\text{wt}(T)} \tag{2}$$

$$= \sum_{\substack{\mu \preceq \nu \preceq_{n-1} \lambda \\ T_1 \in \text{VST}(\nu/\mu) \\ T_2 \in \text{VST}(\lambda/\nu)}} z_1^{\text{wt}(T_1)} (z_2, \ldots, z_n)^{\text{wt}(T_2)} \tag{3}$$

$$= \sum_{\mu \preceq \nu \preceq_{n-1} \lambda} \left(\sum_{T_1 \in \text{VST}(\nu/\mu)} z_1^{\text{wt}(T_1)} \right) \left(\sum_{T_2 \in \text{VST}(\lambda/\nu)} (z_2, \ldots, z_n)^{\text{wt}(T_2)} \right) \tag{4}$$

$$= \sum_{\mu \preceq \nu \preceq_{n-1} \lambda} j_{\lambda/\nu}(z_2, \ldots, z_n) j_{\nu/\mu}(z_1). \tag{5}$$

All that remains is to show that for a fixed $\mu \preceq \nu \preceq_{n-1} \lambda$, we have that $j_{\nu/\mu}(z_1) = z_1^{m-k}(1 + z_1)^{|\nu/\mu| - m + k}$, where k gives the number of $i \in [m]$ such that $\nu_i = \mu_i$.

By definition, we have that

$$j_{\nu/\mu}(z_1) = \sum_{S \in \mathfrak{S}_{\nu/\mu}} wt(S). \tag{6}$$

Because $\mu + \rho$ determines the arrows on the bottom row and $\nu + \rho$ determines the arrows on the first row, and because our lattice model contains the Ice Rule as well as fixed boundary conditions, there is only one

possible valid state in the lattice model corresponding to ν/μ. Thus $j_{\nu/\mu}(z_1)$ is simply the products of the weights in that state.

We stipulate that $\mu \preceq \nu$, so in particular $\mu \subseteq \nu$. In the setting of a lattice model, this tells us that the ith arrow pointing up in the $\mu + \rho$ row, counting from the right starting at 0, is either directly below or below and to the right of the ith arrow pointing up in the $\nu + \rho$ row. Since we have m paths, and k of those paths are such that they travel straight up (whenever $\mu_i = \nu_i$), then we must traverse $m - k$ vertices which have weight z_1, contributing z_1^{m-k} to the product.

On the other hand, we get a weight of $1 + z_1$ whenever a path travels left through a vertex. Since there are $\nu_i - \mu_i$ horizontal segments between every $\mu_i + \rho_i$ entry column and $\nu_i + \rho_i$ exit column, a path entering at $\mu_i + \rho_i$ must travel left through $\nu_i - \mu_i - 1$ vertices before exiting at $\nu_i + \rho_i$, contributing a weight of $(1 + z_1)^{\nu_i - \mu_i - 1}$. However, whenever $\nu_i = \mu_i$, the respective path contributes no such weight (as opposed to a weight of $(1 + z_1)^{-1} = \frac{1}{1+z_1}$), and thus when considering the product of the weights traversed by all m paths, we add a k to the power. We therefore have

$$j_{\nu/\mu}(z_1) = z_1^{m-k}(1 + z_1)^{|\nu|-|\mu|-m+k} \tag{7}$$

allowing us to conclude the equality in Proposition 4.1.

$\square$

Corollary 4.1. *For any $i \in [n]$, we have*

$$j_{\lambda/\mu}(z_1, \ldots, z_n) = \sum_{\mu \preceq_{n-i} \nu \preceq_i \lambda} j_{\lambda/\nu}(z_{i+1}, \ldots, z_n) j_{\nu/\mu}(z_1, \ldots, z_i)$$

Proof. Notice that the proof of Proposition 4.1 could be reproduced by first fixing a SSYT of shape λ/μ with numbers in $[n]$ and then splitting the tableau into two smaller VSTs, one of shape λ/ν filled with numbers in $\{i+1, \ldots, n\}$ and the other of shape ν/μ filled with numbers in $\{1, \ldots, i\}$. The rest of the proof follows. Thus we may choose any available row on which to place the arrows corresponding to $\nu + \rho$ and still get a branching rule. $\square$

5 Attempts at Generalizing our Lattice Model to J_λ

We wish to use our $j_{\lambda/\mu}$ lattice model to demonstrate a lattice model proof of the Cauchy identity in [12]. To do so, we examine look towards finding a lattice model for the weak symmetric Grothendieck polynomials J_λ, the family dual to j_λ, which will be compatible with the lattice model given in Section 3. Here "compatible" means that we want to concatenate the two models together in a way that the resulting system will allow us to calculate both sides of a Cauchy identity between the $J'_\lambda s$ and the $j'_\lambda s$.

In [9], Motegi and Scrimshaw constructed a lattice model whose partition function gives the symmetric Grothendieck polynomial G_λ. Yeliussizov showed in [11] that we can relate symmetric Grothendieck polynomials G_λ with weak symmetric Grothendieck polynomials J_λ via the following change of variables.

Proposition 5.1 (Yeliussizov). *For a partition λ,*

$$J_\lambda(z_1, z_2, \ldots, z_n) = G_\lambda\left(\frac{z_1}{1 - z_1}, \frac{z_2}{1 - z_2}, \ldots, \frac{z_n}{1 - z_n}\right).$$

These two results inspire the following corollary.

Corollary 5.1. *Given any lattice model for symmetric Grothendieck polynomials G_λ, we may construct an analogous lattice model for symmetric Grothendieck polynomials J_λ via the change of variables $z_i \mapsto \frac{z_i}{1-z_i}$.*

Thus, our search for a lattice model for J_λ can be reduced to finding an analagous lattice model for G_λ. This is desirable, as J_λ involves a summation over an infinite set of multiset-valued tableaux, while G_λ involves only a summation over a finite set of set-valued tableaux.

The Motegi-Scrimshaw lattice model for G_λ is not a top-bottom model, as it involves paths entering through the side and exiting the top. As a result, there are certain restrictions on the model that are not

in our j_λ model. The number of variables (row spectral parameters) is fixed to be the number of rows in λ. Additionally, there is no generalization of G_λ to apply to skew partitions λ/μ. To lift these restrictions, we look towards finding a top-bottom lattice model for G_λ that will be compatabile with our $j_{\lambda/\mu}$.

Consider the lattice model for G_λ introduced by Motegi and Scrimshaw in [9]. In the proof of this lattice model, a bijection between SSYTs and states in the lattice model (similar to our j model) is established. In particular, for a particular SSYT of shape λ, and its corresponding lattice model state, the following equivalence is shown.

Proposition 5.2. *(Motegi, Scrimshaw) Let λ be a partition, and let $\mathfrak{T}$ be a SSYT of shape λ with corresponding lattice model state S. Let $SVT(\mathfrak{T})$ denote the collection of set valued tableaux generated by $\mathfrak{T}$ as follows:*

For every box in $\mathfrak{T}$, call the value of the box i.

- *Let K be the set of numbers $j \in [n]$ such that $j > i$, j is at most the value of the box to the right, and j is less than the value of the box below (upholding the semistandard property).*

- *Then, we may generate $2^{|K|}$ SVTs by choosing to include or omit any of the elements of K.*

Then,

$$wt(S) = \sum_{T \in SVT(\mathfrak{T})} z^{wt(T)}$$

Since the weights of this lattice model draw only from the set $\{0, 1, z_i, 1 + z_i\}$, these are exactly the factors of $\sum_{T \in SVT(\mathfrak{T})} z^{wt(T)}$.

Proposition 5.3. *There are no top-bottom lattice models for G_λ satisfying the following conditions:*

- *given a λ, the boundary conditions are fixed*

- *ICE holds, with a 5 vertex model*

- *horizontal lattice lines are in direct correspondence with variables $z_1, ..., z_n$*

- *we have a bijection between SSYTs and states in the lattice model such that for a state S and corresponding SSYT T, $\sum_{SVT(T)} z^{wt(T)} = wt(S)$.*

- *intersecting paths are necessary*

Proof. First, note that if a bijection between SSYTs and states in the lattice model exist, then any weights must be factors of $\sum_{T \in SVT(\mathfrak{T})} z^{wt(T)}$. Moreover, to represent every SSYT generated polynomial, we must use the most indecomposable factors. Thus, the weights of the vertices must draw from the set $\{0, 1, z_i, 1 + z_i\}$.

Suppose such a lattice model exists. WLOG, we will choose the direction of paths to go up and left. For a single path through the lattice model, there are four possible vertices: β_1, β_2, β_3, β_4 (see Figure 8).
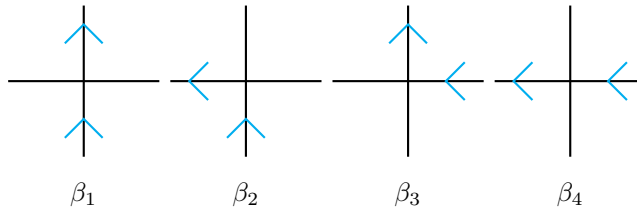

Figure 8: Possible path configurations

We use the following two facts to prove our result.

Fact 1: $1 + z_i$ must be a weight. Otherwise we will only ever have one term (monomial) in our product (the weight of the lattice state).

Fact 2: β_4 must have weight z_i. Consider the tableau of shape $\lambda = (3)$ in one variable. This corresponds to the polynomial z_1^3. So, the lattice model needs at least three on-path vertices on lattice line z_1. Since a path cannot go down, this path must stay on z_1 for at least 3 vertices before leaving. If $wt(\beta_4) \neq z_i$, then it is impossible to obtain z_1^3 (we want one term total, so weights must be either 1 or z_i. If $wt(\beta_4) \neq z_i$, then $wt(\beta_4) = 1$ for a nonzero path. There are only two other vertices on lattice line z_1, and they cannot together contribute z_1^3).

We break into two cases depending on whether the weight of β_2 is zero or nonzero.

Case 1: $wt(\beta_1) = 0$. From Fact 1, we know one of $\beta_1, \beta_2, \beta_3, \beta_4$ must have weight $1 + z_i$.

a: $wt(\beta_2) = 1 + z_i$

The distinguishing problem: Consider the SSYT of shape $\lambda = (1)$ with filling 3. The polynomial corresponding to this SSYT is z_3. So, the path corresponding to this SSYT must reach row 3, crossing all rows less than 3. Since it cannot cross directly vertically (as $wt(\beta_1) = 0$), this creates some sort of zig-zag pattern moving up the lattice model (a β_2 vertex for each line < 3). However, these rows are now undesirably counting towards the polynomial with terms z_j for $j < 3$. This is a contradiction. The argument follows analogously for general i, for $i > 1$.

b: $wt(\beta_3) = 1 + z_i$

Fails base case. Consider the tableau of shape $\lambda = (1)$ in one variable. This of course corresponds to the polynomial z_1. However, any top/bottom path through the lattice model with one variable will have at least one β_3 vertex, giving us more than one term, a contradiction.

c: $wt(\beta_4) = 1 + z_i$

This will not work because β_4 must contribute z_i to the weight of the state.

Case 2: $wt(\beta_1) \neq 0$

Note that if all our weights are nonzero, we have a 6 vertex model, which will immediately increase the number of nonzero states in our lattice model, making it impossible to have a bijection between nonzero states and valid SSYTs. Since we have accepted the fact that intersections are necessary, that vertex is nonzero. Moreover, all off-path vertices must also be nonzero. So, one of $\beta_1, \beta_2, \beta_3, \beta_4$ must have weight 0.

Thus, there are no such lattice models for G_λ.

a: $wt(\beta_2) = 0$

This would be very restrictive. A path can never turn left. All paths must go straight up and have weight $\prod_{i=1}^{n}(wt(\beta_1))$. Since there exists polynomials that are not just monomials, we must have $wt(\beta_1) = 1 + z_i$. However, now the state is only a product of $(1 + z_i)$ terms, giving us an extra term of 1. This is impossible, as no SSYT has weight 1.

b: $wt(\beta_3) = 0$

This is similar to the above case. Once a path is going left, it can never turn up. Since all paths must exit at the top, paths can never turn left, and this is reduced to case **a**.

c: $wt(\beta_4) = 0$

This cannot happen, as Fact 2 asserts that $wt(\beta_4) = z_i$.

$\square$

6 Puzzle Tilings and Littlewood Richardson Coefficients

In this section we introduce puzzles, which in our context are combinatorial objects counted by the coefficients in Littlewood-Richardson style expansions for families of symmetric functions. We then explore possibilities for overlaying paths on puzzles, which allow us to reinterpret puzzles as lattice models.

6.1 Puzzles

A puzzle is a region of honeycomb grid with labelled exterior edges. We fill a puzzle with tiles whose edges are labelled in such a way that the entire interior of the puzzle is filled and the labels along common edges of adjacent tiles are the same. The boundary conditions and types of tiles allowed varies between variations of puzzles. In this subsection, we will discuss one particular choice of boundary conditions with two possible sets of tiles allowed.

To determine the boundary conditions for these two types of puzzles, we require three partitions λ, μ, and ν that fit inside an ambient rectangle of size $k \times (n - k - 1)$. We associate with each partition a binary string obtained by taking the path from the top right corner of the box to the bottom left corner along the boundary of it's Ferrer's diagram, appending a 0 for each horizontal segment and a 1 for each vertical segment. For example an example of how to extract the binary string of a partition, see Figure 9.

Figure 9: Partition $(7, 5, 5, 2) = 010011000100$, inside an ambient rectangle of size $k \times (n - k - 1)$, where $k = 4$ and $n = 12$.

The binary strings are placed along the sides of an equilateral triangular region of side length n of a honeycomb grid to form a $\Delta^{\nu}_{\lambda\mu}$ puzzle as in Figure 8.

Figure 10: Puzzle of size 5 with boundaries shown.

6.1.1 KTW Tiles for Schur Polynomial Littlewood-Richardson Coefficients

Recall the Littlewood-Richardson expansion for Schur polynomials:

$$s_\lambda(\underline{z})s_\mu(\underline{z}) = \sum_{\substack{\nu \\ |\nu| = |\lambda| + |\mu|}} c^{\nu}_{\lambda\mu} s_\nu(\underline{z}). \tag{8}$$

The coefficients $c^{\nu}_{\lambda\mu}$ are called the **Littlewood-Richardson coefficients** for the Schur polynomials.

Puzzles were originally introduced [5] as a combinatorial object counted by the Littlewood-Richardson coefficients for Schur polynomials. In their original form, they used only the following triangular and tetrahedral tiles:
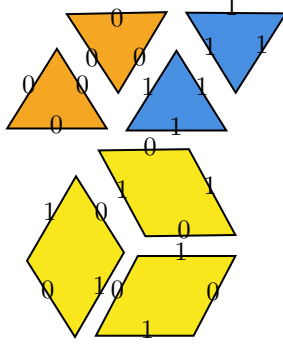
Figure 11: KTW tiles [5]

6.1.2 PY Tiles for Dual Weak symmetric Polynomial Littlewood-Richardson Coefficients

In [10], Pylyavskyy and Yang considered puzzles with an additional tile, the green hexagon:
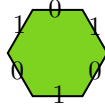

Figure 12: Green hexagon tile(PY), and the three other K-theoretic tiles

[10] showed that with the addition of this new tile, the number of tilings of the puzzle with specific boundary conditions $\Delta_{\lambda\mu}^{\nu}$ were counted by the Littlewood-Richardson coefficients for dual weak symmetric Grothendieck polynomials, $d_{\lambda\mu}^{\nu}$.

There also exists a Littlewood-Richardson style expansion for dual weak symmetric Grothendieck polynomials:

$$j_{\lambda}(\underline{z})j_{\mu}(\underline{z}) = \sum_{\substack{\nu \\ |\nu| \leq |\lambda| + |\mu|}} (-1)^{|\nu| - |\lambda| - |\mu|} d_{\lambda\mu}^{\nu} j_{\nu}(\underline{z}). \tag{9}$$

The coefficients $d_{\lambda\mu}^{\nu}$ are called the Littlewood-Richardson coefficients for the dual weak symmetric Grothendieck polynomials.

We now introduce some terminology useful in understanding the above result.

Definition 6.1. *For some tableau T, define the **reverse row word** of T, denoted row(T), to be the sequence of values of T, read row by row, top to bottom, right to left. The **content** of T is the tuple $(m_1, m_2, \ldots, m_k)$, where m_i is the number of occurrences of i in the sequence row(T).*

Definition 6.2. *A tableau T is **ballot** if in every initial segment of row(T), the number j occurs at least as many times as the number $j + 1$.*

Definition 6.3. *An **inner corner** of the Young diagram of a partition λ is a box whose removal results in the Young diagram of a partition.*

Theorem 6.1 (Pylyavskyy-Yang, Theorem 3.10, Theorem 3.3)**.** *Let λ, ν, μ be partitions such that $|\nu| \leq |\lambda| + |\mu|$, and let λ^- be λ with some number (possibly zero) of inner corners removed. Then, the number of green hexagon tilings with boundary $\Delta_{\lambda\mu}^{\nu}$ is exactly the number of semistandard ballot set-valued tableaux of shape ν/λ^- with content μ.*

Lemma 6.1. *The number of green hexagons in any green hexagon tiling with boundary conditions $\Delta_{\lambda\mu}^{\nu}$ is given by $|\lambda| + |\mu| - |\nu|$.*

Proof. This follows directly from the previous theorem. From each semistandard ballot set-valued tableau of shape ν/λ^- with content μ, circle all numbers in boxes corresponding to removed inner corners of λ. Then,

circle all but the smallest number in each of the boxes corresponding to ν/λ. Note that this method always leaves exactly $|\nu| - |\lambda|$ uncircled numbers. Given that we have content μ, we have precisely $|\mu| - (|\nu| - |\lambda|) = |\lambda| + |\mu| - |\nu|$ circled numbers. From the bijection in Theorem 6.1, these circled numbers correspond exactly to green hexagon tiles in the puzzle. □

6.2 Adding Paths to Puzzle Tilings

Another way to encode the information of puzzles involves the use of paths, which allows us to replace the condition of matching edge labels with the condition of paths matching up across tile boundaries. In the next subSection, we will interpret these paths as states in a lattice model, with the goal of giving a lattice model proof of the Littlewood-Richardson rule.

6.2.1 Paths on KTW Tilings

In [13], Zinn-Justin assigns paths to the triangle and parallelogram tiles introduced above in the following ways:
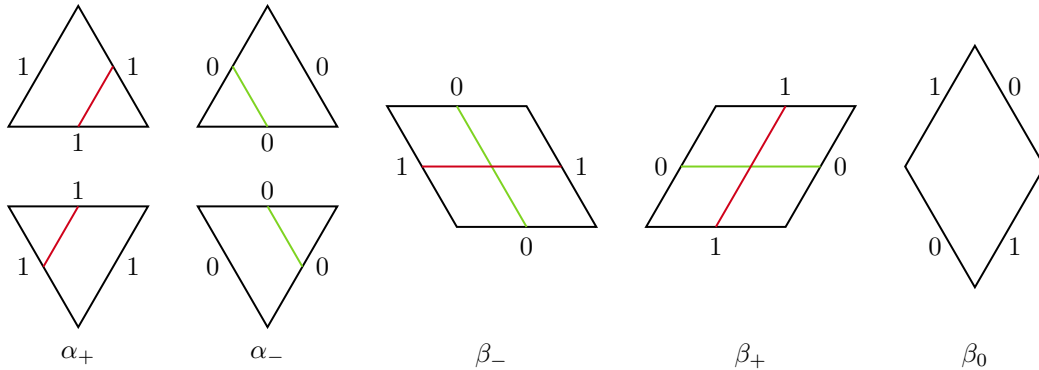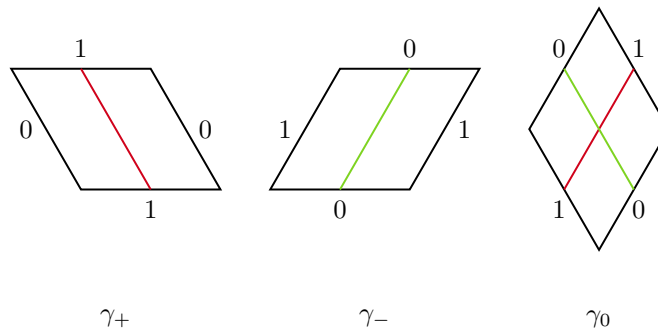

Figure 13: ZJ tiles [13]

We replace Zinn-Justin's $+$ label with 1, and the $-$ label with 0 to align with the tiles from [5].

6.2.2 Paths on PY Green Hexagon Tilings

To incorporate green hexagons into the path model, we consider the $\gamma_{\pm 0}$ tiles from [13], as we cannot tile a green hexagon with the usual $\alpha_{\pm}$ and $\beta_{\pm 0}$ tiles.

By inspection, we see that the only possible ways to tile a green hexagon with the tiles $\{\alpha_{\pm}, \beta_{\pm 0}, \gamma_{\pm 0}\}$ are the following:
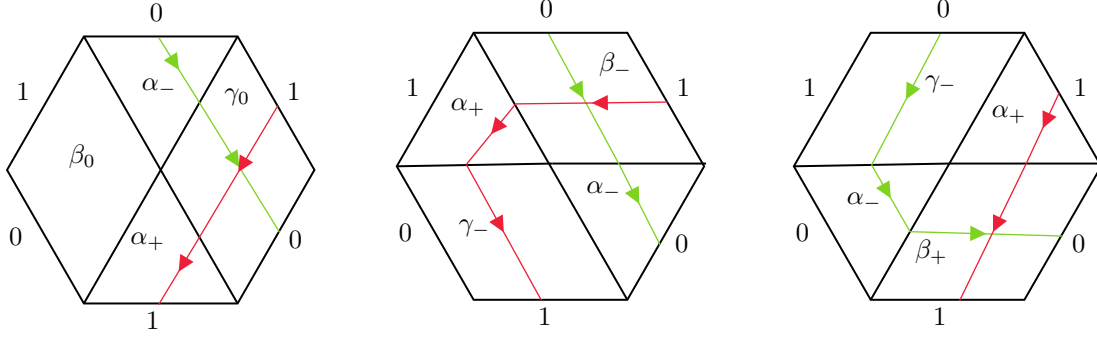
Figure 14: Possible tilings of a green hexagon using the ZJ tiles

In order to maintain the property that green paths travel down and to the right while red paths travel down and to the left, we chose to enforce the leftmost option, restricting our attention to $\{\alpha_\pm, \beta_{\pm 0}, \gamma_0\}$ tilings

Although we may add paths to a green hexagon tiling by replacing the $\alpha_\pm, \beta_{\pm 0}$ of KTW with the path tiles of ZJ and introducing ZJ's γ_0 tile so that we can tile every green hexagon as in the leftmost tiling of Figure 15, the number of $\alpha_\pm, \beta_{\pm 0}, \gamma_0$ tilings is actually greater than the number of green hexagon tilings. Instead, to maintain a bijection between green hexagon tilings and path-tilings, we can use the following set of tiles, in addition to $\alpha_\pm, \beta_{\pm 0}$, which are clearly forced to be placed together in a hexagonal region along with a β_0 of the honeycomb grid wherever they appear. Additionally, note that to maintain a bijection with the green hexagon tilings of [10], we must include $\gamma_0', \alpha_+', \alpha_-'$ (Figure 15).
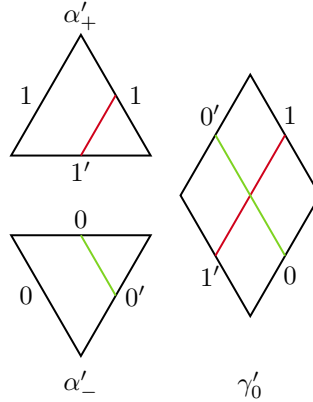

Figure 15: When the above three tiles are added to the usual ZJ tile set of $\alpha_\pm, \beta_{\pm 0}$, the number of tilings of $\Delta_{\lambda\mu}^\nu$ is equal to $d_{\lambda\mu\nu}$.

6.3 Interpreting Puzzles with Paths as Lattice Models

An **MS puzzle** [13] is a rhombus-shaped puzzle where three sides encode Young diagrams and the fourth side, on the upper right, is a sequence $1^{n-k}0^k$ read from bottom to top. In particular, we will be working with MS puzzles which have μ on the bottom left edge, λ on the bottom right, and ν on the top left, written as binary strings of length n from bottom to top on each edge (see Figure 16). Using the set of ZJ tiles $\{\alpha_-, \alpha_+, \beta_{\pm 0}\}$, it is shown in [13] that:
(1) In the top half of the MS puzzle, green paths only move in straight lines ending at the ν boundary; and
(2) The horizontal diagonal of the MS puzzle is also ν, from left to right.
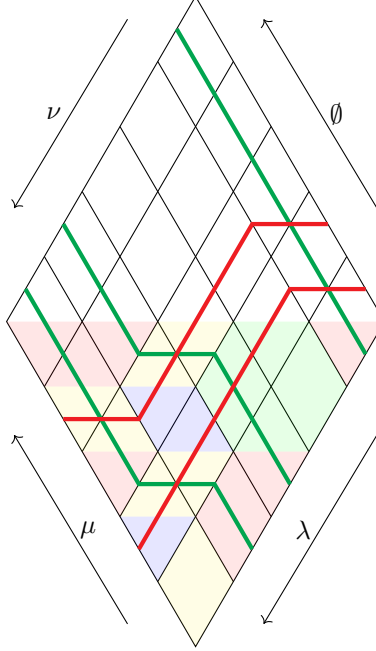
Figure 16: An example MS puzzle

In Section 6.2 of [13], Zinn-Justin describes a bijection between equivariant triangular puzzles and rhombus-shaped MS puzzles, by showing that the top half of the rhombus is fixed and that the bottom half is exactly an equivariant triangular puzzle with boundary conditions $\Delta_{\lambda\mu}^{\nu}$ that has been rotated by $180°$. In a similar vein, we show that we can imbed an equivariant triangular puzzle uniquely in an MS puzzle with the following lemma:

Lemma 6.2. *A triangular puzzle tiling allowing $\{\alpha_-, \alpha_+, \beta_-, \beta_+, \beta_0, \gamma_0\}$ tiles can be uniquely represented as a rhombus-shaped MS puzzle in the following manner:*

1. Rotate the tiled puzzle $180°$, so the tip is pointing down, and attach a triangle of the same size pointing up to the base to get a rhombus.
2. Set the upper left boundary to ν and the upper right boundary to $\emptyset$.
3. Knowing the green paths pass through 0 edges and the red paths pass through 1 edges, tile the remainder of the upper half of the rhombus in the only possible way.

Proof. Rotating a triangular puzzle tiling forces the bottom half of the resulting rhombus. Thus, every triangular puzzle gives exactly one possible rhombus-shaped MS puzzle. Refer to Figure 12. Extend the green paths in straight lines up and to the left until they hit the upper left boundary of the rhombus. $\square$

Note that the above lemma does not give a bijection between triangular puzzles and MS puzzles.
We hope to extend this to a bijection in the future.
The top half of the rhombus-shaped MS puzzle serves as an extension of the triangle puzzle tiling. Hence, it does not encode any information that is not already known from the bottom half of the MS puzzle.

Lemma 6.3. *Any $n \times n$ rhombus-shaped MS puzzle can be written as an $n \times n$ lattice model.*

Proof. Notice that n^2 distinct, vertically oriented rhombi fit on the MS puzzle. Allow each rhombus to represent a vertex on our lattice model. We identify the edges of the rhombus with the incident edges of the vertex; if there is a red (or green) path that hits the edge of a rhombus, the corresponding edge in the lattice model is colored red (or green). For an example of such a translation between a rhombus and a vertex see Figure 17 below:
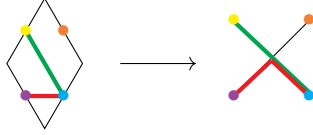
$\square$

Figure 17: The correspondence between rhombic Sections of a puzzle and vertices of a lattice model
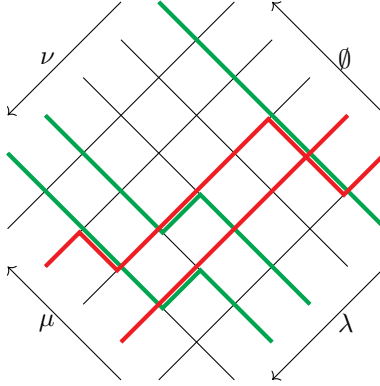

Figure 18: Interpretation of the tiling from Figure 16 as a lattice model. Each tiling of an individual rhombus gives the edge labels of a vertex in our lattice model.

7   Future Work

Recall that in Section 5 we proved a negative result regarding the existence of a lattice model for the weak symmetric Grothendieck polynomials under certain assumptions that we took to be standard lattice model assumptions, although a nonstandard lattice model for these polynomials does exist. Motivated by the third skew-Cauchy identity given in Corollary 6.3 of [12], we had hoped to glue together the lattice model we constructed in Section 3 and a lattice model for the weak symmetric Grothendieck polynomials such that we could compute the partition function of the glued lattice model in two different ways and obtain the desired identity. The difficulty in doing such a gluing construction resided in the fact that the lattice model whose partition function gives $J_\lambda(t_1, \ldots, t_k)$ requires paths to enter from the side and exit out the top, unlike our top-bottom lattice model for $j_{\lambda/\mu}(z_1, \ldots, z_n)$. We hoped that a top-bottom lattice model for $J_\lambda(t_1, \ldots, t_n)$ would make such a gluing construction easier, but concluded that no such lattice model exists, motivating our negative result.

However, [3], a lattice model proof for a Cauchy identity for the LLT polynomials of Lascoux, Leclerc, and Thibon was constructed by gluing together a top-bottom model and a side-top model. This gives us hope that such a lattice model proof exists for the J/j Cauchy identity we wanted, and hence we would like to keep working on finding such a lattice model proof in the future.

On another note, given a λ, μ, and ν, we would like to find a set of Boltzmann weights on the vertices in our lattice model from our MS puzzle in Section 6.3, such that given a certain choice of spectral parameters, the partition function of our lattice model gives $d_{\lambda\mu}^\nu$, the modified Littlewood Richardson coefficients related to our dual weak symmetric Grothendieck polynomials. Having done that, we hope to attach our lattice model from 6.3 to our lattice model from Section 3 and an anti-path model that is a closely related reconfiguration of the latter, and have the models satisfy a Yang-Baxter equation.

Finally, recall that when we replaced the the $\alpha_\pm, \beta_{\pm,0}$ KTW tiles with the path tiles of ZJ and introduced ZJ's γ_0 tile so that we can tile every green hexagon as in Figure 14, the number of possible puzzle tilings can be greater than the number of green hexagon tilings, although we do not know by how many tilings. We fixed this problem in Section 6 by introducing new tiles that are almost identical to the $\alpha_\pm, \gamma_0$ tiles but which contain a prime label that forces our desired green hexagons. We hypothesize that the number of tilings that allow free use of γ_0 is correlated with the number of green hexagons that may appear in a given

green hexagon tiling, but much work is required in this direction to formulate a more precise conjecture.

References

[1] Ben Brubaker, Daniel Bump, and Solomon Friedberg, *Schur Polynomials and the Yang-Baxter equation*, 2010.

[2] Ben Brubaker, Claire Frechette, Andrew Hardt, Emily Tibor, and Katherine Weber, *Frozen Pipes: Lattice Models for Grothendieck Polynomials*, 2020.

[3] Sylvie Corteel, Andrew Gitlin, David Keating, and Jeremy Meza, *A vertex model for LLT polynomials*, 2020.

[4] Michael Curran, Calvin Yost-Wolff, Sylvester Zhang, and Valerie Zhang, *Ribbon Lattices and Ribbon Function Identities (preprint)*, (2019).

[5] Allen Knutson, Terence Tao, and Christopher Woodward, *The honeycomb model of $GL(n)$ tensor products II: Puzzles determine facets of the Littlewood-Richardson cone*, Journal of the American Mathematical Society **17** (2004), no. 1, 19–48.

[6] Thomas Lam and Pavlo Pylyavskyy, *Combinatorial Hopf algebras and K-homology of Grassmanians*, 2007.

[7] A. Lascoux and M. Schützenberger, *Symmetry and flag manifolds*, 1983.

[8] Alain Lascoux and S Ole Warnaar, *Branching rules for symmetric functions and sln basic hypergeometric series*, Advances in Applied Mathematics **46** (2011), no. 1-4, 424–456.

[9] Kohei Motegi and Travis Scrimshaw, *Refined dual Grothendieck polynomials, integrability, and the Schur measure*, 2020.

[10] Pavlo Pylyavskyy and Jed Yang, *Puzzles in K-homology of Grassmannians*, Pacific Journal of Mathematics **303** (2019), no. 2, 703–727.

[11] Damir Yeliussizov, *Duality and deformations of stable Grothendieck polynomials*, Journal of Algebraic Combinatorics **45** (2016), no. 1, 295–344.

[12] Damir Yeliussizov, *Symmetric Grothendieck polynomials, skew Cauchy identities, and dual filtered Young graphs*, 2018.

[13] Paul Zinn-Justin, *Littlewood–Richardson coefficients and integrable tilings*, arXiv preprint arXiv:0809.2392 (2008).